Characteristics of zircon in placer deposits along the west coast of South Africa

C. Philander[a], A. Rozendaal[a*] and R.J. de Meijer[b]

Mining along the west coast of South Africa is dominated by the exploitation of onshore and offshore diamond deposits. The relatively recent discovery of vast resources of heavy minerals in the area has resulted in the establishment of a major related industry. Today, Namakwa Sands is a 10-million-ton-per-year operation and significant producer of ilmenite, zircon and rutile by world standards. Heavy minerals are widely distributed along the entire west coast and are mainly concentrated in Mesozoic fluvial, Cainozoic marine and Recent aeolian unconsolidated placers. Basement rocks form part of the middle to late Proterozoic Namaqualand Metamorphic Complex, Gariep Group and Palaeozoic Cape Supergroup. Their diverse lithologies are the source of the younger heavy-mineral concentrations.

The present study focuses on the characteristics of zircon ($ZrSiO_4$), the mineral with the highest intrinsic value of the entire heavy-mineral suite. Both the heavy-mineral fraction and zircon concentrates of a representative suite of samples along the west coast were investigated using analytical techniques that included: transmitted/reflected light microscopy, electron microprobe mineral analysis, ICP for rare earth element analyses, PIXE for single-grain analyses and cathodoluminescence. Their radiometric characteristics were determined using a hyper-pure germanium detector.

All samples studied comprised a heterogeneous population of zircon grains with diverse physico-chemical properties. This was expressed by large differences in colour and trace element chemistry of single grains. The percentage of grains hosting inclusions, such as ilmenite, magnetite, monazite, quartz and fluids, varied for each sample. Zoned, metamict and grains with overgrowths and replacement textures contributed to the diverse characteristics of zircon samples. Concentrations of the various grain types differed among samples and contributed to the unique character of each population. Bulk chemistry and radiometric signature support this observation. This variation depends on the composition of the source rock and stage of sedimentological evolution of the sands. A high degree of heterogeneity of the zircon population will adversely affect beneficiation of these mineral deposits. As a result, its quantification is required to optimize mineral recovery.

The discovery of diamonds at the beginning of the century drew interest to the Namaqualand coast and, since then, mining along the west coast of South Africa has been dominated by the successful exploitation of onshore and offshore diamond deposits. However, in recent years the emphasis has shifted from exclusive diamond mining and exploration to include exploration for heavy minerals.

The coastal plain of the west coast of South Africa is marked by widespread heavy mineral deposits. These are related to classical placers set in fluvial, marine and aeolian environments. The heavy mineral deposits include garnet, zircon, pyroxene, ilmenite and other opaques as major constituents with amphiboles, rutile and kyanite present in minor or trace amounts. Exploration for heavy minerals during the 1980s resulted in the discovery of several deposits of which one, the Namakwa Sands deposit at Graauwduinen (Fig. 1), proved economically viable. Namakwa Sands has resources of an estimated 500 Mt at a grade of 10 % total heavy minerals and mines 10 Mt per annum. Today, it is a significant producer of high quality zircon, ilmenite and rutile.[1]

Zircon, which has the general chemical formula $ZrSiO_4$, usually contains a range of elements in subordinate or trace amounts substituting for Zr and Si in the crystal lattice. In most instances these trace elements are considered impurities and decrease the quality of the zircon concentrate and therefore its nett worth. In addition, mineral, fluid and gas inclusions contribute to the heterogeneity of this mineral. As a result, variability in the physico-chemical characteristics of zircon as well as its alteration products have an adverse influence on the recoverability of the mineral in conventional separation plants.

Although several studies have been

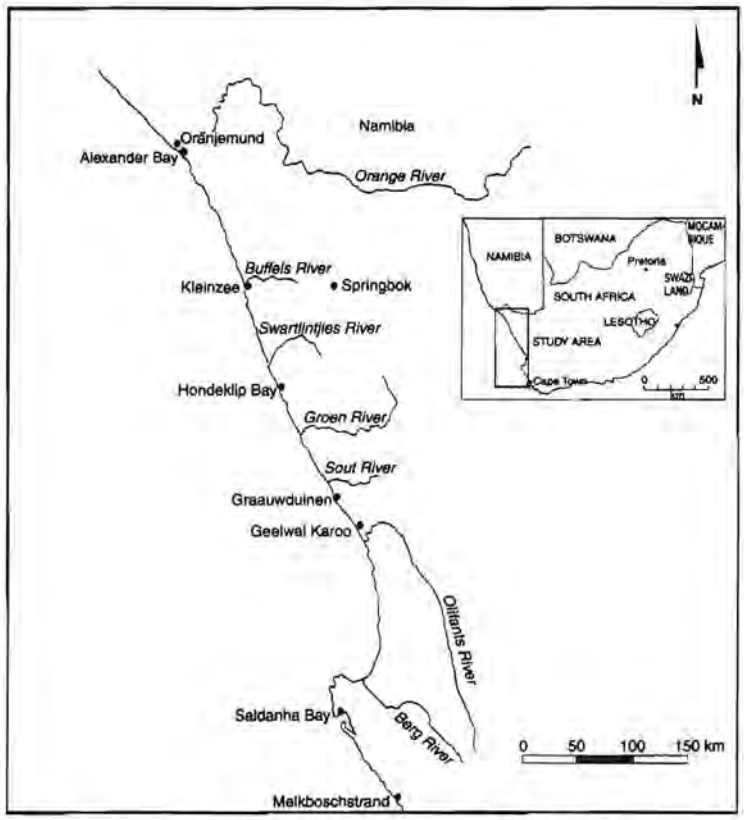

Fig. 1. Locality map of the study area along the west coast of South Africa.

[a]Department of Geology, University of Stellenbosch, Private Bag X01, Matieland, 7602 South Africa.
E-mail: 9001670@narga.sun.ac.za

[b]Nuclear Geophysics Division, Kernfysisch Versneller Instituut, Rijksuniversiteit Groningen, Zernikelaan 25, 9747 AA Groningen, The Netherlands.
E-mail: demeijer@kvi.nl

*Author for correspondence. E-mail: ar@maties.sun.ac.za

conducted on the characteristics and mineralogy of the heavy-mineral fraction of west coast deposits, limited attention was devoted to the zircon fraction.[1-4] This investigation demonstrates the diversity of zircon concentrates in placer deposits. A multi-disciplinary approach was followed using a variety of physical and chemical methods, which included transmitted/reflected light microscopy, electron microprobe analysis, inductively coupled plasma-atomic emission spectrometry (ICP-AES) for rare earth element (REE) analyses, radiometric analysis, particle-induced X-ray emission (PIXE) for single-grain analyses and cathodoluminescence spectroscopy.

Geological setting

The west coast of southern Africa between Saldanha Bay and Oranjemund is rocky and generally straight with a few local embayments and prominent headlands (Fig. 1). It is backed by the 'Great Escarpment,' a topographical feature that runs for 100 km parallel to the coast and a 3–6-km-wide coastal plain that rises gently to a maximum height of 100 m.[5] This semiarid, Namaqualand coastal plain is drained by numerous rivers, of which only the seasonal Orange, and Krom, a tributary of the Olifants, cross the escarpment.

The regional geology of the Namaqualand coast consists of Cainozoic to Recent sediments deposited mainly on Precambrian basement.[6-9] The latter includes diverse lithologies from the mid-Proterozoic Namaqualand Metamorphic Complex, late-Proterozoic Gariep Group and Palaeozoic Cape Supergroup. Early Miocene, clay-filled fluvial channels form along the coast and are locally associated with high concentrations of diamonds.[10-12] Pleistocene to Pliocene diamondiferous marine deposits overlie the coastal channels and occur as a number of wave-cut, raised marine terraces consisting of basal gravels, overlain by a succession of marine and aeolian sands.[13,14]

Heavy minerals, defined as the mineral fraction of sands with a density >2.9, are concentrated in semi-consolidated sands of palaeo- and recent strandlines and overlying dunefields. The combined effects of littoral drift, wave action and sections of J-shaped bays controlled the anomalous local concentration of heavy minerals along the coast. In some areas, these minerals constitute up to 90 % of the total in these sands. High-grade metamorphosed basement rocks are considered the most important source of these minerals. Several marine and aeolian cycles of sediment reworking have concentrated the heavy mineral population.[2]

Methods

A representative suite of samples of the various sedimentological environments along the coast was collected from Melkboschstrand in the south to Oranjemund in the north. The suite consisted of four basic groups, which included palaeo-fluvial (Group A), present-day beach (Group B), aeolian sands (Group C) and present-fluvial (Group D). Samples were first washed in de-ionized water and the heavy mineral fraction separated from the 63–250-μm sieve fraction in bromoform (relative density 2.90). A relatively uncontaminated zircon fraction was obtained using a Frantz isodynamic separator with a side slope of 25° and forward tilt of 15°. A series of settings ultimately exceeding 1.5 A was used to remove the magnetically susceptible fraction and produced a zircon-rutile concentrate. Rutile and other constituents were removed by subsequent panning. Finally, single grains were handpicked under a binocular microscope to obtain an unmixed zircon fraction. This was a source of samples for polarized-light microscopy, microprobe analyses, PIXE analyses, SEM-EDS studies and cathodoluminescence (CL). Another fraction was powdered, treated with 8 N HCl and dissolved for REE determination. Radiometric analyses were performed on the total concentrate. Monazite was removed by diluted HCl.

Selected carbon-coated grains were examined by combined SEM-EDS to semi-quantify geochemistry and verify optical observations. The SEM also provided a means of studying texture within single grains. Back-scattered electron (BSE) images allowed location of distinct chemical zones within grains that otherwise displayed a homogeneous optical character. Luminescent images were acquired using an Oxford Instruments MonoCL system attached to a Leitz Analytical S440 SEM with an electron-beam energy of 15 kV and beam current of 2.1 nA. Zircons were also studied in a Cameca Camebax electron microprobe microanalyser at the Department of Geochemistry, University of Cape Town. Accelerating voltage was 15 kV with a beam current of 40 nA measured at the Faraday cup. Radiometric analysis was performed at the Kernfysisch Versneller Instituut, Groningen, the Netherlands. The equipment uses a high-sensitivity gamma-ray detector using a pure germanium scintillator crystal.[15,16] REE analyses for U, Th, La, Ce, Pr, Nd, Sm, Eu, Gd, Dy, Ho, Er and Yb were carried out by ICP-AES at the Physics Department, University of Stellenbosch. The ICP equipment was operated at 1.0 kW forward power and a plasma gas flow rate of 15.0 l min^{-1} and 1.5 l min^{-1} for the auxiliary gas.

Results

Physical characteristics

All four sample groups contained zircons that varied in size from 75–180 μm; larger grains of up to 250 μm occurred in Group A. Their colour was extremely variable.

Although the colourless to pink variety dominated, some displayed shades of yellow to brown and also orange to purple. Some grains were frosted, a feature caused by abrasion and etching during fluvial and marine transport. Metamict zircons in particular showed a range of colours from light grey to yellow and brown. The zircons of Group A were mainly light pink to colourless with yellow and metamict varieties present in minor to trace amounts. Colourless zircons dominated the populations of Group B (present-day beach) and Group C (aeolian). By contrast, the zircons from the riverine environment (Group D) showed a wide variety of colours with yellow to yellow-brown dominating. Fielding[17] suggested that strong colours are associated with the presence of U and supports the conclusions of Matumura and Koga[18] that colour centres are related to Zr^{3+} produced by radiation-induced reduction of Zr^{4+}.

Most zircons appeared as rounded to spherical grains more numerous than idiomorphic crystals. Distinctly zoned grains with complex internal structures were also present. Group D zircons were mainly distinctive euhedral crystals comprising a variety of crystal forms and habit, whereas Groups A, B and C contained more rounded grains, with poorly crystalline faces. Irregularly shaped, angular fragments were more common in Group D.

Cracks radiating from the centre had developed in many grains and were a typical feature of metamict zircons, particularly common in Group D. Speer[19] suggested that this feature arises from the radioactivity of Th and U present as substitution elements in the zircon crystal lattice. Opaque spots are believed to form when atoms are forced from the crystal by radioactive emissions from U and Th,

leaving vacant positions in the crystal lattice that subsequently leads to crystal shattering.

Inclusions were common, comprising spherical and tabular gas/fluid types, transparent crystals, opaque phases and their combinations. Tabular inclusions were often elongated parallel to crystallographic axes whereas others showed no preferred orientation. Solid inclusions confirmed by EDS included ilmenite, rutile, biotite, muscovite, titanite, apatite, monazite, xenotime, REE-silicate (allanite), Al-silicate (sillimanite), feldspar, quartz and several unidentified phases. Inclusions of small, euhedral zircon crystals, often orientated parallel to the *c*-axis, were noted and confirmed by EDS. The larger zircons hosted the most inclusions, of which Ilmenite formed the largest and most common, closely followed by apatite.

Cathodoluminescence

Cathodoluminescence displayed by zircons can be primarily attributed to transitions of Dy^{3+} ions, defects in the zircon crystal lattice (specifically those localized on SiO_4 tetrahedra), and also by the presence of small amounts of Nd, Mn, Ho, Tm, Yb and Lu.[20-23] Other elements such as Fe, Hf, Y, P and U act as quenchers and suppress luminescence.[24,25] Thus, the relative intensity of light emission depends on the quantity and types of activators and quenchers.[26]

Although most zircons appear structureless in plane-polarized or reflected light, CL spectroscopy revealed complex internal structures (Fig. 2). A variety of types were identified in the experimental sample:

I. Zircon that was either homogeneously weak or brightly luminescent and sometimes passed into a peripheral overgrowth with contrasting luminescence.
II. Grains that showed a patchy distribution of nonuniform luminescence throughout the crystal. A thin, bright overgrowth marked the rim.
III. Grains that displayed narrowly spaced, oscillatory growth zones. More than one region of such growth was commonly present and revealed by a difference in luminescence. The overall luminescence of the different regions decreased towards the rim. Cores were rarely observed and rims were marked by a bright overgrowth. Cracks radiating from the core indicated metamict zircons.
IV. Zircon similar to type III, but a well-defined core was present that overprints the surrounding oscillatory zones. Occasionally the different oscillatory zones replaced each other. A thin, very luminescent rim overgrowth was observed.
V. Grains similar to type IV but in addition contained secondary growth zones with differing luminescence that surrounded and replaced the oscillatory zones from the outside of the crystal. A well-defined bright overgrowth marked the rim. The cores and growth zones were marked by a well-preserved resorption surface.
VI. Grains with a prominent core, surrounded by one or more concentric growth zones of contrasting luminescence and, if present, a brighter rim. These zircons had a distinct boundary between the core and subsequent overgrowth; each region gave a distinctive CL emission.
VII. Zircon similar to type VI but the core replaced the surrounding brighter phases of growth. A bright rim overgrowth was present.

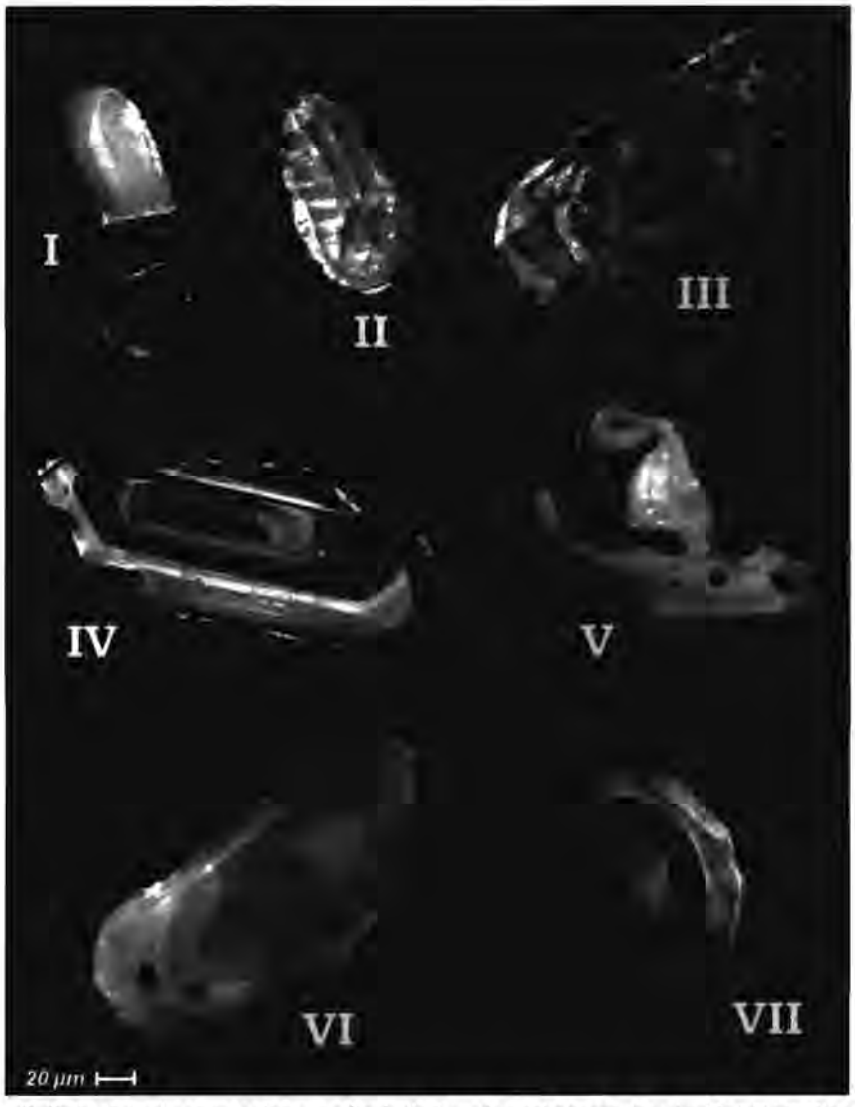

Fig. 2. Cathodoluminescence images of selected west coast zircons (see text for description of types).

The zircons displayed complex CL spectra demonstrating their variable trace element chemistry and protracted evolution. Few grains displayed similar characteristics across the entire population sampled.

Geochemistry

The chemical formula of zircon is $ZrSiO_4$, but a range of trace elements can be incorporated in the crystal lattice through coupled substitution. Zr^{4+} is commonly replaced by Hf^{4+}, U^{4+}, Th^{4+}, Y^{3+}, REE^{3+} ($La \rightarrow Lu$), Nb^{5+}, Ta^{5+}, Ti^{4+}, Pb^{4+}, Pb^{2+}, Fe^{3+}, Fe^{2+}, Ca^{2+}, Na^{+} and K^{+} and Si^{4+} by Al^{3+}, P^{5+} and S^{6+}.[19] It is also possible that these trace elements are present as inclusions of separate mineral phases.

Microprobe analyses were performed on a representative suite of zircons for Si, Zr, Hf, Al, Fe, K, Ca, Y, P, Th and U. The results are presented in Table 1 as averages

Table 1. Average chemistry of zircons in the various groups.

		Si	Zr	Hf	Y	P	Th	U	Ca	Mg	Fe	K	Total
Group A ($n = 33$)	$\bar{x}$	32.35	65.06	1.30	0.15	0.04	0.03	0.01	0.01	0.01	0.02	0.01	99.01
	s.d.	0.48	0.95	0.13	0.12	0.04	0.03	0.01	0.01	0.01	0.01	0.01	0.90
Group B ($n = 54$)	$\bar{x}$	32.39	65.78	1.29	0.04	0.02	0.01	0.00	0.00	0.00	0.03	0.01	99.59
	s.d.	0.15	0.61	0.05	0.01	0.00	0.00	0.00	0.00	0.00	0.00	0.01	0.73
Group C ($n = 55$)	$\bar{x}$	31.55	64.96	1.90	0.12	0.31	0.02	0.01	0.01	0.01	0.03	0.01	99.11
	s.d.	1.36	2.09	0.35	0.28	0.71	0.01	0.01	0.01	0.01	0.01	0.01	1.94
Group D ($n = 33$)	$\bar{x}$	32.07	66.36	1.51	0.21	0.08	0.00	0.00	0.00	0.00	0.06	0.00	100.35
	s.d.	0.43	0.78	0.16	0.12	0.06	0.00	0.00	0.00	0.00	0.02	0.00	0.74

Detection limit = ±0.05 wt %.

Table 2. REE data for zircons in Groups A, B and C.

Sample	La	Ce	Pr	Nd	Sm	Eu	Gd	Dy	Ho	Er	Yb	ΣREE
A1	504	833	74	179	26	3	46	116	40	165	223	2210
A2	200	345	35	111	23	4	58	132	47	170	215	1340
A3	280	429	41	120	20	4	41	124	41	173	235	1506
B1	62	106	7	37	13	3	35	106	35	144	263	811
B2	36	60	3	19	13	5	70	217	68	288	328	1106
B3	43	75	3	21	13	5	70	216	67	278	321	1110
B4	69	108	4	28	16	4	68	229	70	304	328	1229
C1	34	58	6	20	11	3	37	110	40	161	316	796
C2	35	58	6	20	12	4	39	128	43	180	334	858
C3	48	82	10	36	21	7	59	167	52	210	380	1072

Normalized data

Sample	La	Ce	Pr	Nd	Sm	Eu	Gd	Dy	Ho	Er	Yb	La/Yb
A1	2059	1306	767	378	171	60	223	458	705	995	1351	1.25
A2	818	541	363	234	149	74	286	520	829	1023	1300	0.53
A3	1144	672	421	253	130	67	199	486	729	1044	1421	0.68
B1	252	166	68	78	84	59	171	416	615	868	1595	0.18
B2	147	95	27	40	82	82	343	854	1200	1733	1986	0.06
B3	176	117	29	44	86	80	344	848	1174	1674	1943	0.08
B4	282	169	44	60	102	76	335	902	1235	1833	1984	0.10
C1	137	90	62	43	73	59	181	433	699	972	1912	0.10
C2	142	90	64	43	80	65	193	503	751	1082	2020	0.09
C3	195	128	99	77	134	126	291	655	919	1266	2301	0.12

for each group. The compositional differences among zircons from the different groups were slight. Those from Groups A and B had on average 32.35 wt % Si, 65.06 wt % Zr and 1.31 wt % Hf. Zircons from Group C had Zr values of 64.96 wt % and a relatively elevated Hf content of 1.90 wt %. Group D displayed a slightly lower Hf content.

The Hf-Zr relationships among zircons of the various groups are illustrated in Fig. 3. Minor elements include Y, P, Th and Fe and are not particular to any specific group. Most of the concentrations were very close to the detection limit of the instrument. Semi-quantitative SEM data, supported by PIXE analyses, showed that the strongly coloured zircons were relatively enriched in Fe and Al, particularly in Group D. Trace amounts of K, Ca and Mg were also detected. Within the constraints of the electron microprobe, no

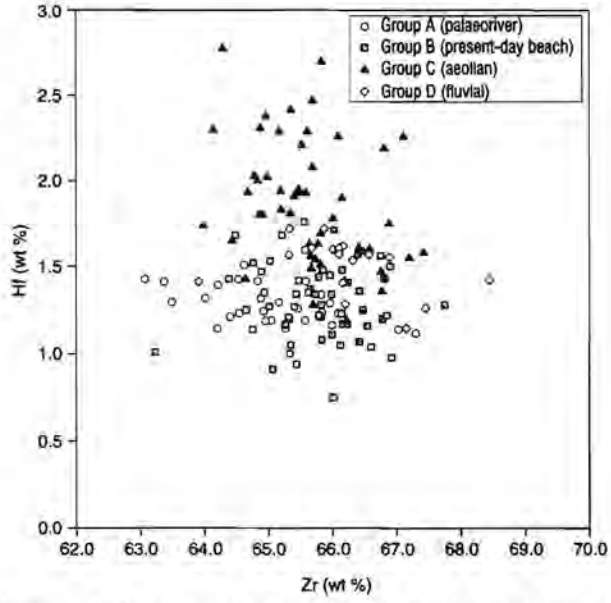

Fig. 3. Binary diagram of hafnium/zirconium relationship of zircons from the various groups along the west coast.

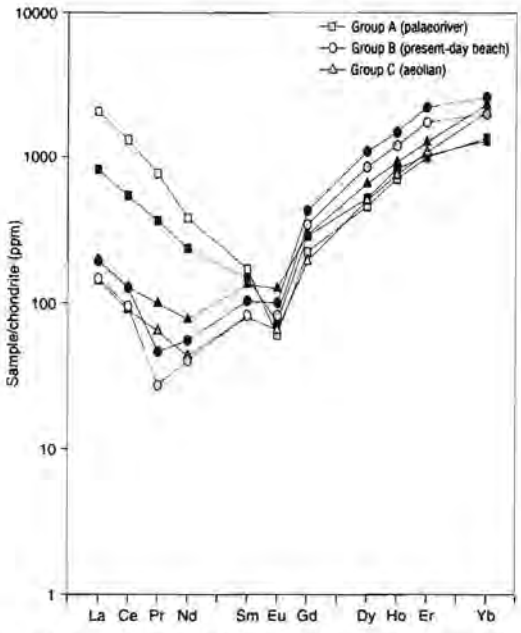

Fig. 4. REE patterns for Group A ($n = 3$), B ($n = 4$) and C ($n = 3$) zircons.[28]

consistent correlation between colour and chemistry was established.

The results of REE analysis of pure zircon concentrates are listed in Table 2 and graphically represented as chondrite normalized values after Evensen in Fig. 4.[28]

In addition, a La/Yb index was calculated that reflected which of the LREE and HREE dominated the REE profile. The La/Yb ratio is calculated as

$$\frac{La + Ce + Pr + Nd + Sm}{Gd + Dy + Ho + Er + Yb}$$

The total REE content of Group A zircons ranged from 1340–2210 ppm. The chondrite-normalized patterns had a typical 'birdwing' distribution, symmetrical about Eu. These zircons were characterized by prominent LREE- and HREE-enriched profiles, well-defined Eu anomaly and the absence of a Ce anomaly. La/Yb values showed that, except for one case, the zircons of Group A were relatively enriched in the HREE with respect to the LREE. The HREE profiles were notably smooth with a minor change of slope at Dy. The LREE pattern resembles a steep, straight line.

Group B zircons had a total REE content considerably lower than those in Group A. Generally, these zircons had a steep HREE and a moderate LREE-enriched profile, slight Eu anomaly and a negative anomaly at Nd. The La/Yb ratios were much lower than those in Group A.

The total REE content of zircons in Group C was slightly lower but comparable with Group B zircons. It displayed similar normalized profiles, but instead of a Nd anomaly, a negative anomaly at Pr was present. La/Yb values were similar to those for Group B, ranging from 0.10–0.12. The REE profiles showed that zircons from the different depositional environments had their own distinctive chemistry.

Radiometry

The activity (C) of ^{40}K and gamma-ray-emitting nuclei in the ^{238}U and ^{232}Th decay series were measured radiometrically. The results for the different groups are depicted in Fig. 5, in which the activity of Th and Bi is shown. Zircons from Group B plot in a very tight field that is marked by the lowest C_{Bi} and C_{Th} values of all the groups. Group C zircons clustered close to Group B, but Groups A and D had distinctly different characteristics. The latter's elevated radiometric signatures reflect greater U and Th content. They also had very different REE profiles from the other groups.

The radiometric character of each group was distinctive and related to their differences in sedimentary environment, provenance and maturity. For example, an immature sediment in a contemporary fluvial environment has a zircon population that consists of stable and unstable grains with respect to physico-chemical characteristics. The unstable component commonly includes zircons that are cracked, metamict and contain high concentrations of Hf, Th, U and other trace elements. As the sediment ages during consecutive recycling events, the unstable component is progressively removed to produce a mature deposit such as beach sand with a stable zircon population. This relationship is clearly reflected in the radiometric signatures and chemistry of the four groups studied. The 'immature' group D zircons from young fluvial systems are distinctly different from the older beach and aeolian sands that have been subjected to many cycles of reworking. Geochemical and radiometric analysis of zircons can therefore be used to discriminate between the sedimentary environment, provenance and maturity of their hosts.

Conclusions

- A variety of analytical techniques have shown that the zircon population in each group is heterogeneous with regard to physical and chemical properties.
- The zircons can be discriminated by size, colour, and morphological features such as crystal habit and form.
- Generally, west coast zircons have stoichiometric proportions of Zr and Si. Minor to trace amounts of Hf, Fe, Al, Fe, Y, P, U, Th and REE substitute for Zr and

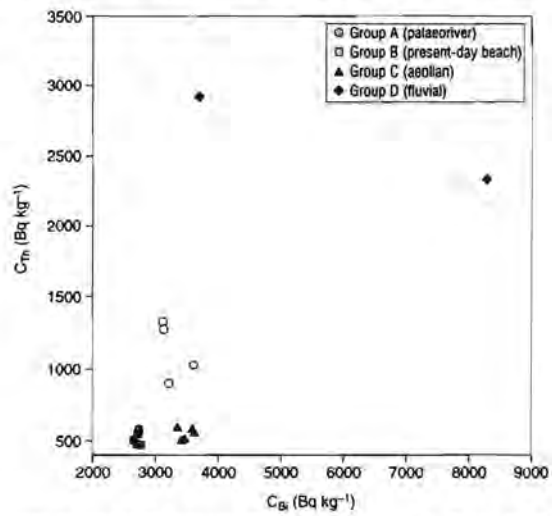

Fig. 5. Radiometric activity plot of C_{Th} against C_{Bi} for Group A ($n = 4$), B ($n = 5$), C ($n = 5$) and D ($n = 2$) zircons.

Si in the crystal lattice. In addition, mineral inclusions also contribute small, but significant amounts of impurities to the composition.

- CL spectra demonstrated the great complexity of single zircons. The several types of zoning have significance with respect to Hf, U and Th distribution in the crystal lattice.
- Although major element chemistry indicates only subtle differences among the four groups studied, contrasting trace element chemistry, REE and radiometric characteristics indicate that the west coast zircons from particular geological environments are distinct. Group A is associated with a palaeofluvial environment, Group B with a present-day beach, Group C with an aeolian placer and Group D with a contemporary river.
- Samples dominated by strongly coloured zircons show high Bi-Th activities and were enriched in U, Th, Fe, Hf, Y and Al, whereas colourless zircons had reduced Bi-Th activities and possessed a notably lower trace element concentration.
- Zircons from the Richards Bay Minerals (RBM) deposit in northern KwaZulu-Natal displayed similar major element chemistry but had U, Th, Hf, REE and Bi-Th concentrations several orders of magnitude higher than those from the west coast. RBM zircons are generally colourless to pink, but metamict and yellow varieties make up a considerable component. Abundant inclusions with a diverse chemistry are present in nearly all zircons.[27] These differences indicate contrasting provenance terrains.
- Heterogeneity of the zircon population from the various locations and geological environments influences its recovery in conventional mineral separation plants. Zircons that are relatively enriched in Hf, U, Th and REE together with those that contain abundant ilmenite inclusions have increased electromagnetic and conductive susceptibility compared to a homogeneous, purer zircon. Impure zircons will be removed early in the electromagnetic and conductive cycles and consequently could amount to a considerable loss in the separation process. This loss of zircon could adversely affect the economic viability of mining operations.
- It is therefore necessary to quantify the zircon populations in both the plant-feed and tailings to have better control of recovery.
- With prior knowledge of zircon properties in a placer deposit, plant conditions can be adjusted to yield maximum recovery of a product required to meet particular specifications.
- REE and radiometric analyses of zircon could prove useful in provenance discrimination as they demonstrate differences that can be related to the nature of the sedimentary source.

We thank R. O' Brien for REE analysis and D. Gurneycke for SEM and cathodoluminescence studies. Microprobe analyses were performed by D. Rickard.

1. Palmer G.L. (1994). The discovery and delineation of heavy mineral sand orebodies at Graauwduinen, Namaqualand, Republic of South Africa. *Exploration in Mining Geology* **3**, 399–405.
2. Macdonald W.G. and Rozendaal A. (1995). The Geelwal Karoo heavy mineral deposit: a modern day beach placer. *African Journal of Earth Science* **21**, 187–200.
3. Macdonald W.G., Rozendaal A. and De Meijer R.J. (1997). Radiometric characteristics of heavy mineral-deposits along the west coast of South Africa. *Mineralium Deposita* **32**, 371–381.
4. De Meijer R.J., Stapel C., Jones D.G., Roberts P.D., Rozendaal A. and Macdonald W.G. (1997). Improved and new uses of natural radioactivity in mineral exploration and processing. *Exploration in Mining Geology* **6**, 105–117.
5. Heydorn A.E.F. and Tinley K.L. (1980). Estuaries of the Cape: Part I: synopsis of the Cape coast, natural features, dynamics and utilization. CSIR Research Report 380, Pretoria.
6. De Villiers J. and Sohnge P.G. (1959). Geology of the Richtersveld. *Mem. Geol. Surv. S. Afr.* **48**, 1–295.
7. Hallam C.D. (1964). The geology of the coastal diamond deposits of southern Africa (1959). In *The Geology of Some Ore Deposits in Southern Africa*, ed. S.H. Haughton. Geological Society of South Africa, pp. 671–728.
8. Pether J. (1986). Late Tertiary and early Quaternary marine deposits of the Namaqualand coast, Cape Province: new perspectives. *S. Afr. J. Sci.* **82**, 464–470.
9. Woodborne M.W. (1986). The Seafloor Geology of the Namaqualand Inner Shelf between White Point and Stompneus Bay (Diamond Concession Area No. 4). *Rep. Geol. Surv. S. Afr.* 1986-0077, 1–21 pp.
10. Carrington A.J. and Kensley B.F. (1969). Pleistocene molluscs from the Namaqualand coast. *Ann. S. Afr. Mus.* **52**, 189–223.
11. Rogers J., Pether J., Moleneux R., Genis G., Kilham J.L.V., Cooper G. and Corbett I.B. (1990). Cenozoic geology and mineral deposits along the west coast of South Africa and the Sperrgebiet. In *Guidebook Geocongress '90*, Geological Society of South Africa, Johannesburg.
12. Siesser W.G. and Dingle R.V.D. (1981). Tertiary sea-level movements around southern Africa. *J. Geol.* **89**, 83–96.
13. Dingle R.V., Siesser W.G. and Newton A.R. (1983). *Mesozoic and Tertiary Geology of Southern Africa*. Balkema, Rotterdam.
14. Pether J. (1994). *The sedimentology, palaeontology and stratigraphy of coastal-plain deposits at Hondeklip Bay, Namaqualand, South Africa*. M.Sc. thesis, University of Cape Town.
15. Greenfield M.B., De Meijer R.J., Put L.W., Wiersma J.F. and Donahue J.F. (1989). Monitoring beach sand transport by use of radiometric heavy minerals. *Nuclear Geophysics* **3**, 231–244.
16. De Meijer R.J., Lesscher H.M.E., Schuling R.D. and Elburg M.E. (1990). Estimate of the heavy mineral content in sand and its provenance by radiometric methods. *Nuclear Geophysics* **4**, 455–460.
17. Fielding P.E. (1970). The distribution of uranium, rare earths and colour centres in a crystal of natural zircon. *American Mineralogist* **55**, 428–440.
18. Matumara O. and Koga H. (1962). On colour centres in $ZrSiO_4$. *J. Phys. Soc. Jap.* **17**, 409.
19. Speer J.A. (1980). In *Orthosilicates*, ed. P.H. Ribbe. *Mineral. Soc. Am., Rev. Mineral.* **5**, 67–112.
20. Mariano A.N. (1988). Some further geologic applications of cathodoluminescence. In *Cathodoluminescence of Geologic Materials*, pp. 94–123, ed. D.J. Marshall. Unwin Hyman, Boston.
21. Mariano A.N. (1989). Cathodoluminescence emission spectra of rare earth element activators in minerals. In *Geochemistry and Mineralogy of Rare Earth Elements*, eds B.R. Lipin and G.A. McKay. *Mineral. Soc. Am., Rev. Mineral.* **21**, 339–348.
22. Yang B., Luff B.J. and Townsend P.D. (1992). Cathodoluminescence of natural zircons. *J. Phys. Condens. Matter* **4**, 5617–5624.
23. Vasconcellos M.A.Z., Chemale L.T. and Steele I.M. (1996). Zircon zonation: an experimental study using electron probe microanalysis, cathodoluminescence spectroscopy and synchrotron X-ray fluorescence. *International Conference on Cathodoluminescence and Related Techniques in Geosciences and Geomaterials.*
24. Hanchar J.M. and Miller C.F. (1993). Zircon zonation patterns as revealed by cathodoluminescence and back-scattered electron images: implications for interpretation of complex crustal histories. *Chem. Geol.* **110**, 1–13.
25. Hanchar J.M. and Rudnick R.L. (1995). Revealing hidden structures: the application of cathodoluminescence and back-scattered electron imaging to dating zircons from lower crustal xenoliths. *Lithos* **36**, 289–303.
26. Koschek G. (1993). Origin and significance of the SEM cathodoluminescence from zircon. *J. Microscopy* **171**, 223–232.
27. Pietersen K.J. (1993). *Richards Bay zircon*. M.Sc. thesis, University of Natal.
28. Evensen M.N. (1978). Rare-earth abundances in chondritic meteorites. *Geochem. Cosmochim. Acta* **42**, 1203.